



# GNSS scale determination using calibrated receiver and Galileo satellite antenna patterns

Arturo Villiger<sup>1</sup> · Rolf Dach<sup>1</sup> · Stefan Schaer<sup>1,2</sup> · Lars Prange<sup>1</sup> · Florian Zimmermann<sup>3</sup> · Heiner Kuhlmann<sup>3</sup> · Gerhard Wübbena<sup>4</sup> · Martin Schmitz<sup>4</sup> · Gerhard Beutler<sup>1</sup> · Adrian Jäggi<sup>1</sup>

Received: 13 December 2019 / Accepted: 6 August 2020  
© The Author(s) 2020

## Abstract

The reference frame of a global terrestrial network is defined by the origin, the orientation and the scale. The origin of the ITRF2014 is defined by the ILRS long-term solution, the orientation by no-net rotation conditions w.r.t. the previous reference frame (ITRF2008), and the scale by the mean values from global VLBI and SLR solution series (Altamimi et al. in *J Geophys Res Solid Earth* 121:6109–6131, 2016). With the release of the Galileo satellite antenna phase center offsets (PCO) w.r.t. the satellites center of mass (GSA in Galileo IOV and FOC satellite metadata, 2019) and the availability of new ground antenna calibrations for GNSS receivers, based on anechoic chamber measurements or on robot calibrations, GNSS global network solutions qualify to contribute to the scale determination of terrestrial networks, as well. Our analysis is based on global multi-GNSS solutions of the years 2017 and 2018 and may be seen as “proof of concept” for the contribution of GNSS data to the scale determination of the terrestrial reference frame. In a first step, the currently used Galileo PCO estimations (Steigenberger et al. in *J Geod* 90:773–785, 2016) are compared to the released PCO values, which show discrepancies on the decimeter-level. Eventually, the published Galileo PCOs are used in an experimental solution as known values. GNSS-specific PCOs are estimated, as well, for GPS and GLONASS, together with the “standard” parameters set up in global GNSS solutions. From the estimated network coordinates, a time series of daily scale parameters of the terrestrial network is extracted, which shows an offset of the order of 1 ppb (parts per billion, corresponding to a height difference of 6.4 mm on the Earth’s surface) w.r.t. to the ITRF2014 network and an annual variation with an amplitude of about 0.3 ppb.

**Keywords** GNSS antenna calibrations · TRF scale · Disclosed Galileo antenna calibrations

## 1 Introduction

According to the International Earth Rotation and Reference Systems Service (IERS) Conventions (Petit et al. 2010), the realization of a terrestrial reference system (TRS) leading to the corresponding terrestrial reference frame (TRF) includes the definition of:

- the origin of the coordinate system, supposedly the center of mass (geocenter).
- the unit of length (meter).
- the orientation of the coordinate system.
- the time evolution of the orientation (constrained to a list of time-dependent station coordinates by no-net rotation conditions (NNR)).

✉ Arturo Villiger  
arturo.villiger@aiub.unibe.ch

<sup>1</sup> Astronomical Institute of the University of Bern, Sidlerstrasse 5, Bern 3012, Switzerland

<sup>2</sup> Federal Office of Topography (swisstopo), Wabern, Switzerland

<sup>3</sup> Institut für Geodäsie und Geoinformation, Universität Bonn, Bonn, Germany

<sup>4</sup> Geo++, Gesellschaft für satellitengestützte geodätische und navigatorische Technologien mbH, Garbsen, Germany

The realization of the International TRF (ITRF) is based on four space geodetic techniques and is regularly updated by including the most recent data (Altamimi et al. 2016). The underlying techniques are:

- Very Long Baseline Interferometry (VLBI).
- Satellite Laser Ranging (SLR).
- Doppler Orbitography and Radiopositioning Integrated by Satellite (DORIS).

- Global Navigation Satellite Systems (GNSS): So far, only GPS and GLONASS were considered.

One important aspect when realizing a reference frame is the realization of the scale. Up to now, the scale of the ITRF is defined by VLBI and SLR. A priori unknown satellite antenna phase center offsets (PCO) prevented the use of GNSS for the scale estimation. The dynamic GNSS satellite orbits are, w.r.t. to the center of mass (COM), well defined by the laws of celestial mechanics. The GNSS measurements refer, however, to the phase center of the transmitting antenna. They are linked to the COM of the satellites by the PCOs, describing the offset between the COM and the phase center of the antenna. Because the scale and the  $z$ -components of the receiver and the satellite antenna PCOs are strongly correlated (Rebischung 2014; Bruni 2016; Zhu et al. 2003), the scale can only be estimated if calibrations for both, the ground and space segment, are available. An alternative way to reduce the correlation between the two parameter types is to add measurements from Low Earth Orbiters (LEO) into global GNSS analyses (Haines et al. 2015).

The European GNSS Agency (GSA) released as the first system provider the satellite antenna calibrations of the Galileo satellites including PCO and Phase Variations (PV) (GSA 2019). Therefore, the scientific community has no longer to rely on estimates. Up to now only, GPS and GLONASS data were used in the International GNSS Service (IGS, Johnston et al. 2017) contribution to the various ITRFs. With the availability of multi-GNSS calibrations for the ground antennas, by robot (Wübbena et al. 1997, 2000) and anechoic chamber calibrations (Zeimet and Kuhlmann 2008), and by including Galileo to the next IGS contribution for the ITRF, the problem of uncalibrated PCOs and PVs for GPS and GLONASS satellite antennas can be circumvented, offering the potential for GNSS observations to contribute to the scale determination of future ITRF releases.

This article presents the results of a reprocessing effort to assess the potential of GNSS for scale determination using calibrated antenna patterns on the ground and the space segment. When GSA first disclosed the patterns in 2017 for the Galileo In Orbit Validation (IOV) satellites, only chamber calibrations for receiver antennas were available, covering Galileo in addition to GPS and GLONASS. During 2019, in preparation of the IGS contribution to the next ITRF version 2020, Geo++ published a set of robot calibrations including Galileo. To study the impact of the two methods of antenna calibration, a two-year reprocessing was performed twice, once using robot calibrations and once using chamber calibrations only, allowing to study the feasibility of the two methods for scale determination and to analyze the impact of the different calibration techniques.

Section 2 introduces the two antenna pattern calibration techniques. Satellite antenna patterns provided by GSA and

chamber and robot multi-GNSS receiver antenna calibrations are introduced and the available data sets are presented. Section 3 is dedicated to the reprocessing effort which has been performed to assess the potential of the GNSS data to contribute to the scale determination. Section 4 addresses the inner consistency of the antenna calibrations using the so-called inter-system translation biases (ISTP), which introduces for each station an offset for  $x$ ,  $y$ , and  $z$  between the coordinates from GPS and from all other GNSS. The main focus of Sect. 5 is on the scale and PCO estimation. Whenever using the term PCO, we only mean the  $z$ -component.

## 2 Antenna calibrations

Zhu et al. (2003) showed that the satellite antenna PCOs and scale are strongly correlated. Therefore, it is difficult to estimate both values simultaneously. An arbitrary scale for the ground coordinates can be partially absorbed by estimating the satellite PCOs. If the scale is changed by +7.4 parts per billion (ppb) (station height + 5 cm), then this would lead to a satellite PCO change of  $-1$  m and the solution would be still consistent. One way to reduce the correlation between the two parameter types is to introduce additional GNSS measurements from LEO satellites (Haines et al. 2015) or to use calibrated satellite antenna PCOs.

The main problem of previous reprocessing efforts organized by the IGS for ITRF updates was that neither the scale nor the satellite PCOs were known (Ray et al. 2013). The satellite PCOs were adjusted to the ITRF scale based on VLBI and SLR. The corresponding satellite PCOs were estimated and made publicly available (Schmid et al. 2007, 2016). Meanwhile, the situation has changed. New GNSS have been launched and are operational. GSA has released the satellite antenna patterns for all Galileo satellites as the first GNSS provider. The antenna patterns for the regional Quasi-Zenith Satellite System (QZSS) were released by the Cabinet Office, Government of Japan, in 2017 (CAO 2017). Because QZSS is a regional system, its contribution to a global solution is limited. It is, therefore, not used in this study. The next two subsections briefly introduce the satellite antenna calibrations and the available multi-GNSS receiver antenna calibrations (chamber and robot).

### 2.1 Satellite antennas

Before GSA released the Galileo satellite antenna offsets and patterns, the community relied on estimated PCO values (Steigenberger et al. 2016) similar to the case of GPS and GLONASS. The ground antenna patterns for Galileo were adopted from GPS L1 and L2 calibrations. Comparing the released PCOs and the estimated values referring to

**Table 1** Estimated (Steigenberger et al. 2016) and calibrated Galileo satellite antenna PCOs (ionosphere-free linear combination) for the z-component in cm

Satellite	Estimated	Calibrated	Differences
E101 (IOV)	95	83.7	11.3
E102 (IOV)	95	92.4	2.6
E103 (IOV)	95	82.4	12.6
E201 (FOC)	105	90.7	14.3
E202 (FOC)	105	86.4	18.6
E203 (FOC)	110	92.6	17.4
E204 (FOC)	110	75.3	34.7
Average	--	--	15.9

the ionosphere-free (IF) linear combination reveals notable discrepancies (see Table 1).

Note that the estimates from Steigenberger et al. (2016) are rounded to cm. On average, the PCOs for the z-component from the chamber calibrations are about 16 cm smaller than the estimates derived from GNSS data. The main reason could be:

1. Missing antenna calibrations for Galileo for ground antennas. GPS L2 offsets and patterns have been used for the E5a signals due to the lack of available calibrations. If there is a systematic difference between L2 and E5a over all antennas, this discrepancy would influence the satellite PCO estimations.
2. Incompatible scale between GPS and GLONASS (based on the ITRF 2014 scale) on the one hand and Galileo on the other hand. Scale differences would also be partially absorbed by the satellite PCOs.

The Galileo constellation was initiated in 2011 by launching the first two IOV satellites (<https://www.gsc-europa.eu/system-service-status/orbital-and-technical-parameters>, accessed November 21, 2019). Later on, in 2012, two more IOV satellites were launched. The constellation has been systematically augmented with the Full Operational Capability (FOC) satellites and reached its nominal constellation in 2018. The last satellites started to transmit in early 2019. Therefore, there are several years available with an almost full Galileo constellation prior to 2018 and since 2019 the full constellation is available. The next ITRF solution will be based on reprocessed data up to the end of the year 2020 or beyond.

## 2.2 Receiver antennas

As mentioned above, the availability of adequate calibrations is essential for scale determination. Menge et al. (1998) showed that the lack of absolute receiver antenna patterns

**Table 2** Type-mean antenna patterns from chamber (CHA) and robot (ROB) calibrations, the number of individual calibrations contributing to their generation, and the number of IGS sites using the corresponding antenna (status December 11, 2019)

Antenna/Radom		#CHA	#ROB	#sites
AOAD/M_T	NONE	2		25
AOAD/M_T	SCIS	1		
ASH700936A_M	NONE	1		2
ASH700936C	NONE	1		
ASH700936C_M	NONE	5		1
ASH700936D_M	NONE	1		
ASH700936D_M	SCIS		2	1
ASH701945B_M	NONE	1		3
ASH701945C_M	NONE	1	1	8
ASH701945E_M	NONE		1	12
ASH701945E_M	SCIS		1	1
ASH701945E_M	SCIT		1	2
CHCC220GR2	CHCD		5	1
JAVRINGANT_DM	NONE	6	1	19
JAVRINGANT_DM	SCIS		22	17
JAVRINGANT_G5T	JAVC		10	
JAVRINGANT_G5T	NONE	1	6	11
JAV_GRANTG3T	NONE		2	2
JAV_RINGANT_G3T	NONE	25		10
JNSCR_C146221	NONE	5		
LEIAR10	NONE	5	3	7
LEIAR20	LEIM	34	64	5
LEIAR20	NONE	3	8	5
LEIAR25.R3	BEVA	2		
LEIAR25.R3	LEIT	13	1	25
LEIAR25.R3	NONE	1	5	4
LEIAR25.R4	LEIT	63	37	31
LEIAR25.R4	NONE	7	3	9
LEIAS10	NONE	3		
LEIAT502	NONE	1		
LEIAT504	NONE		1	3
LEIAT504GG	NONE		20	6
LEIAX1202GG	NONE	2		1
NAX3G+C	NONE	2		
SEPCHOKE_B3E6	NONE		5	7
SEPCHOKE_B3E6	SPKE		6	10
SEPCHOKE_MC	NONE	2		2
SEPCHOKE_MC	SPKE	2		1
TPSCR.G3	NONE		1	12
TPSCR.G3	SCIS		1	13
TPSCR.G3	TPSH		1	2
TPSCR.G5	NONE	1		
TPSCR.G5	TPSH		29	22
TPSCR.G5C	NONE		5	1
TRM115000.00	NONE		20	14

**Table 2** continued

Antenna/Radom		#CHA	#ROB	#sites
TRM159900.00	SCIS	4		
TRM29659.00	NONE		1	4
TRM55971.00	NONE	1		5
TRM55971.00	TZGD	5	1	1
TRM57971.00	NONE	5	25	26
TRM57971.00	TZGD	53	1	2
TRM59800.00	NONE	10	5	30
TRM59800.00	SCIS	8	6	29
TRM59900.00	NONE	7		
TRM59900.00	SCIS	38	21	3

can result in networks scale differences of up to 1 cm per 1000 km. The antenna calibrations associated with the ITRF 2014 are mainly based on robot calibrations for GPS and GLONASS L1 and L2 observations (Schmid et al. 2016). To take advantage of the satellite antenna calibrations for Galileo, calibrations are needed for the ground network, as well. Chamber-calibrated receiver antennas covering the full spectrum of frequencies provide a potential set of calibrations. In 2019, Geo++ released a first set of robot calibrations including Galileo while preparing the next IGS contribution to the ITRF 2020.

### 2.2.1 Chamber calibrations

Before multi-GNSS robot calibrations became available in 2019, chamber calibrations were the only available source for Galileo E5 antenna patterns. A data set of more than 250 individual patterns were collected and used to create mean antenna calibrations. In total, type-mean calibrations for 36 antenna / random combinations were created (Table 2).

The available receiver antenna calibrations cover about 50% of the IGS sites. For our scale study, this leads to the network shown in Fig. 1 with a total of 183 sites and a subset of 97 sites capable of tracking Galileo (as of January 1, 2017).

### 2.2.2 Robot calibrations

Our analysis is based on 37 robot calibrations (Table 2) including Galileo. Because the igs14.atx antenna model file is based on robot calibrations, the data set has been extended by adding the GPS/GLONASS only calibrations. For data processing, only observations with calibrations were used. If a receiver-tracked Galileo but no corresponding calibrations were available, the observations were skipped. This leads to the network shown in Fig. 2 with a total of 296 sites and a subset of 94 sites capable of tracking Galileo (as of January 1, 2017).

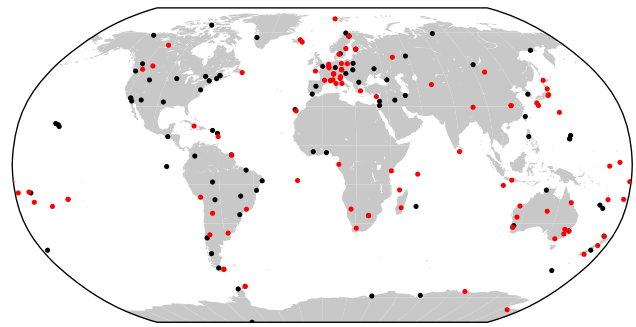


**Fig. 1** Network used in this study for January 1, 2017 using chamber calibrations only. The black dots represent GPS/GLONASS sites, whereas the red dots indicate sites including Galileo

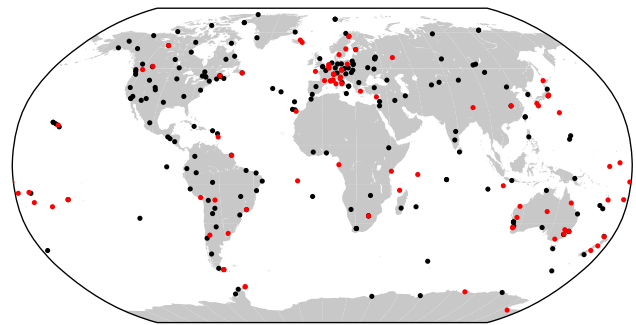


**Fig. 2** Network used in this study for January 1, 2017 using robot calibrations. The black dots represent GPS/GLONASS sites, whereas the red dots indicate sites including Galileo

## 2.3 Comparison

Table 3 lists the PCO up-component for the IF for all systems. For GPS L1/L2, for GLONASS L1/L2, and for Galileo E1/E5 are used. The two data sets are using different datum definitions for their patterns. Applying a zero-mean condition over all PV and removing removal of a constant term allows to compare the calibrations from the two techniques. From Table 3, we conclude that on average the PCOs are consistent within 1 mm. For individual antenna types, however, the differences may reach values up to 7 mm.

## 3 Case study covering 2017 and 2018

To study the potential of using calibrated antennas in space and on ground, data covering the years 2017 and 2018 were processed. The latest IERS and IGS standards were used. Table 4 summarizes the settings.

Our analysis consists of two solutions, one using chamber calibrations and the other one using robot calibrations only for the receiver antennas. The IGS14 antenna model, a collection of robot calibrated type-mean patterns for GPS and GLONASS L1 and L2, was modified replacing 37 GPS/GLONASS antenna patterns with their newly released

**Table 3** Z-PCO of robot and chamber calibrations for the ionosphere-free linear combination (GPS: L1/L2, GLONASS: L1/L2, Galileo: E1/E5) in mm. Datum: Zero-mean condition over PV and constant term removed. ROB: Robot calibrations, CHA: chamber calibrations

Antenna	GPS			GLONASS			Galileo		
	ROB	CHA	ROB-CHA	ROB	CHA	ROB-CHA	ROB	CHA	ROB-CHA
ASH701945C_M NONE	65.73	60.45	5.28	65.95	68.27	-2.32	62.99	56.13	6.86
JAVRINGANT_DM NONE	63.36	65.99	-2.63	63.90	67.21	-3.31	59.96	61.42	-1.46
JAVRINGANT_G5T NONE	46.03	47.92	-1.89	41.32	40.41	0.91	39.46	40.24	-0.78
LEIAR10 NONE	93.00	96.91	-3.91	96.56	100.49	-3.93	90.28	94.20	-3.92
LEIAR20 LEIM	116.68	111.64	5.04	115.60	110.11	5.49	106.68	102.99	3.69
LEIAR20 NONE	113.27	109.86	3.41	113.93	109.01	4.92	103.57	100.25	3.32
LEIAR25.R3 LEIT	156.40	147.37	9.03	158.19	154.99	3.20	151.34	145.31	6.03
LEIAR25.R3 NONE	150.81	144.97	5.84	153.93	150.40	3.53	147.01	144.53	2.48
LEIAR25.R4 LEIT	149.76	150.77	-1.01	151.46	154.10	-2.64	146.48	148.31	-1.83
LEIAR25.R4 NONE	152.08	156.29	-4.21	152.58	157.78	-5.20	148.89	151.93	-3.04
TRM55971.00 TZGD	80.29	82.84	-2.55	77.53	82.48	-4.95	74.74	77.37	-2.63
TRM57971.00 NONE	75.27	77.68	-2.41	73.94	77.93	-3.99	72.74	72.46	0.28
TRM57971.00 TZGD	79.39	80.54	-1.15	77.43	78.18	-0.75	75.03	76.46	-1.43
TRM59800.00 NONE	62.31	60.43	1.88	63.27	61.72	1.55	57.63	58.48	-0.85
TRM59800.00 SCIS	59.87	57.10	2.77	59.98	58.49	1.49	56.96	53.93	3.03
TRM59900.00 SCIS	99.99	104.87	-4.88	101.81	106.16	-4.35	100.30	103.15	-2.85
Mean value	97.76	97.23	0.53	97.96	98.61	-0.65	93.38	92.95	0.43

multi-GNSS calibrations. Therefore, calibrations for all IGS antennas were available leading to the network in Fig. 2 with more than 300 stations. Note that only Galileo observations from receivers with calibrated antennas were used. From the 300 sites, more than 100 covered Galileo at the beginning of 2017. This number steadily grew up to 150 stations by the end of 2018 (Fig. 3). The second solution included only sites covered by the chamber calibrations. This led to a reduced set of about 200 sites. The number of stations including Galileo was almost the same as in the solution with robot calibrations. The number of processed sites over the 2 year time period is shown in Fig. 3 and the network distribution, for January 1, 2017, in Figs. 1 and 2.

### 3.1 Processing strategy

Our study is based on the Center for Orbit Determination in Europe (CODE) GPS and GLONASS Final IGS operational processing (Dach et al. 2017). The processing scheme was extended to include Galileo based on CODE's MGEX solutions (Prange et al. 2020). The processing was performed using the Bernese GNSS software (Dach et al. 2015). Table 4 lists the key characteristics of our processing scheme. The generation of our solution can be divided into two parts. The first part performs the double-difference network solution over one day (24 h). In the second part, the daily solutions are combined into a 3-day solution by combining the underlying 1-day Normal Equations (NEQ). This step stabilizes the

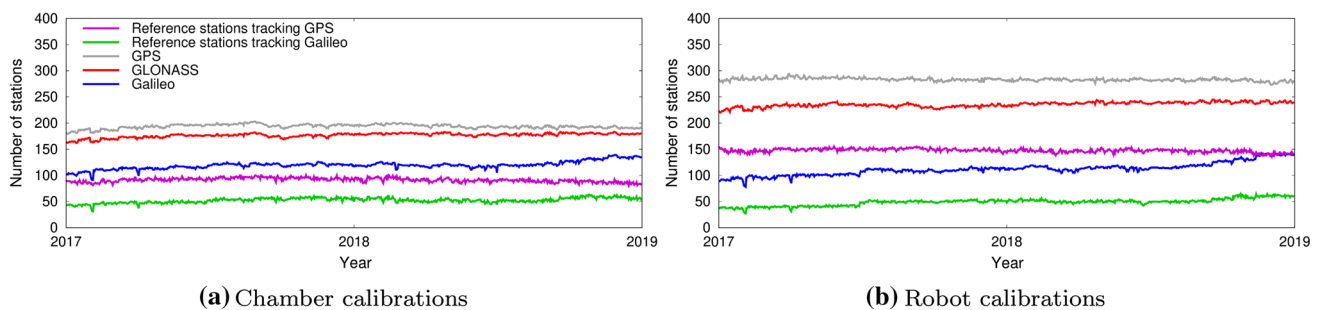
orbits and the Earth Orientation Parameters (EOP) (Lutz et al. 2016). Datum definition is achieved by applying a no-net-translation and a no-net-rotation condition (three translation and three rotation constraints) to a well-defined list of ITRF positions (Altamimi et al. 2016), after having removed outliers, i.e., stations with more than 1 cm horizontal and more than 3 cm vertical differences, from the reference station list (IGS14—the IGS-specific realization of the ITRF2014 (Rebischung and Schmid 2016)). Figure 3 shows the total number of reference stations and reference stations including Galileo for both solutions. The datum of the solution using chamber calibrations is based on average on 100 sites, where 50 of them are tracking Galileo. The solution based on robot calibrations is based on around 150 fiducial sites where 50 track Galileo in analogy to the other solution.

### 3.2 Solutions

Two sets of solutions were produced to study the impact of satellite antenna calibrations. The first set, subsequently labeled as *ROB*, is based on robot calibrations for the receiver antennas. The second set using chamber calibrations for the ground antennas is labeled *CHA*. The number of Galileo satellites grew from 13 to 20, the number of GPS and GLONASS satellites remained stable at 32 and 24 satellites, respectively, for the 2-year test period (Fig. 4).

**Table 4** Processing characteristics according to the latest IERS/IGS standards. Details in Dach et al. (2015)

Setting	Strategy
Observable type	Double-difference, Phase-only ionosphere-free linear combination
Cut-off angle	3°
Sampling rate	180 sec
Observation weighting	Squared cosine of zenith angle ( $\cos^2$ )
Ambiguity resolution	
Melbourne-Wübbena	Up to 6000km (GPS (G)and Galileo (E))
QIF	Up to 2000km (GRE)
Narrow- and wide-lane	Up to 200 (GE)
Direct	Up to 20 km (GRE)
Satellite modeling	
GPS	L1/L2, ECOM2 (Arnold et al. 2015) & albedo (Rodriguez-Solano et al. 2012)
GLONASS	L1/L2, ECOM2 & albedo
Galileo	L1/L5, ECOM2 and Macro-model (GSA 2019) for albedo / solar radiation pressure
Antenna thrust	applied
Troposphere	VMF (2h) (Böhm et al. 2006)
Troposphere gradients	Model: CHENHER (24h, piece-wise linear) (Chen and Herring 1997)
Higher order ionosphere	3 components using CODE's GIM products
Antenna corrections	
Satellite PCO/PV	According to IGS14; Galileo using chamber calibrations from GSA
Receiver PCO/PV	chamber-only or robot-only solution
Earth Orientation Parameter	24 h, x & y components, UT1-UTC at day boundaries
Datum definition	ITRF 2014, minimum constraint (3 translations, 3 rotations)
Fiducial sites	iterative process, outlier rejection (horizontal: > 1 cm; vertical: >3 cm)
Product types	1 day and 3 day (Orbits, ERP, CRD) solutions

**Fig. 3** Number of stations tracking GPS, GLONASS, and Galileo, and number of reference stations including GPS or Galileo and GPS

#### 4 Receiver PCO verification

The scale determination depends on the antenna calibrations. A simple way to test the consistency of the individual antenna patterns is to generate GPS-, GLONASS- and Galileo-only solutions and to compare the resulting coordinates. Ideally, the differences between all coordinate sets would be zero. We used a similar approach by analyzing the observations of all GNSS in the same parameter estimation procedure, and

by setting up so-called inter-system translation parameters (ISTP) in the observation equations (Dach et al. 2015). The ISTPs are offsets ( $x$ ,  $y$ , and  $z$ ) pointing from the GPS to the GLONASS or Galileo phase center of the same site. Because we allow for such a vector for each station, the corresponding satellites of that system can be shifted by an arbitrary value. To avoid such arbitrary shifts, a system-specific datum definition needs to be introduced, in analogy to the geodetic datum. System-dependent multipath effects, potential deficiencies in

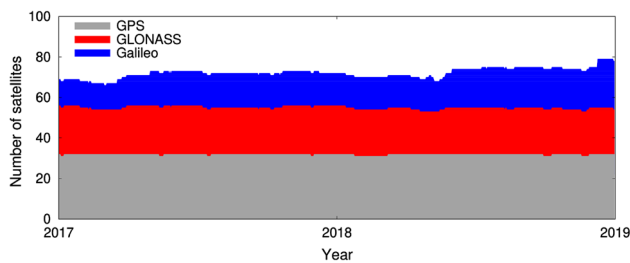


**Fig. 4** Number of processed satellites

the troposphere models, inaccurate receiver antenna calibrations, and other effects may result in non-zero values for the ISTPs. Scale inconsistencies in the individual GNSS satellite PCOs may be absorbed by a common offset for all stations.

Experiment 1a (using the ITRF 2014 scale) introduces ISTPs using six zero-mean conditions, three translations and three rotations for datum definition. A non-zero average of the ISTPs vertical component indicates that the scales of the used satellite PCOs are not consistent among the three systems. A mean offset for Galileo has to be expected and the offsets for GLONASS should be close to zero as the GPS and GLONASS PCOs are aligned to the ITRF2014 scale, whereas the Galileo PCOs are based on chamber calibrations. The main purpose of this experiment is to assess the impact of the inconsistent scale between the ITRF2014 and the chamber-calibrated Galileo satellite antenna pattern on the station coordinates. As opposed to Experiment 1a, the Experiment 1b introduces adjusted PCO values based on a Galileo-induced scale (Sect. 5.2 below). The outcome of the experiment is expected to have no mean offsets in the up component of the ISTPs, as the satellite PCOs of the three systems are mutually consistent. The ISTP values reflect the consistency between the individual type-mean antenna calibrations w.r.t. the overall scale introduced with the Galileo scale. Experiment 2 introduces, in addition to the ISTPs, an elevation- and GNSS-specific Troposphere Bias Parameter (GTRP) using the WET-VMF model (Böhm et al. 2006), w.r.t. GPS. The GTRP accounts for deficiencies in the elevation-dependent PV antenna patterns as well as deficiencies in the troposphere models and system-dependent multipath effects.

## 4.1 Results

Table 5 lists the ITSP and GTRP values of the experiments. Experiment 1a compares the consistency of robot and chamber calibrations w.r.t. current IGS14 antenna models (no changes to GPS and GLONASS, extended by the Galileo PCOs from GSA). The ISTP results reveal, as expected, that the consistency between GPS and GLONASS is better for robot than for chamber calibrations. This seems to be obvious because the GPS and GLONASS PCOs for the satellites

**Table 5** Median ISTP offsets and GTRP where estimated in mm using the IGS14 antenna models (IGS14) and a solution with the adjusted GPS and GLONASS PCOs to be consistent with Galileo (Galileo Scale). The listed ISTPs refer to the up component

Experiment GNSS	Sol.	IGS14	Galileo scale		GTRP
		1a ISTP	1b ISTP	2 ISTP	
GLONASS	CHA	−3.15	−1.11	0.20	−0.46
	ROB	−1.07	−0.91	0.38	−0.49
Galileo	CHA	8.40	0.19	0.59	0.02
	ROB	6.63	1.01	0.05	0.41

were estimated using robot calibrations for the ground antennas. In case of Galileo, we see a clear discrepancy of about  $\pm 7$  mm for both calibration types. This is a result of different scales between the GPS/ GLONASS and Galileo PCO values. The differences between the GLONASS and Galileo ISTPs from robot and chamber calibrations show an average discrepancy of 2 mm. Experiment 1b removes the discrepancy between GPS/ GLONASS and Galileo scale which is reflected in the ISTPs from Experiment 1a. By adjusting PCOs with a system-specific PCO offset for GPS and GLONASS (introducing a Galileo scale), the inconsistency between the different GNSS is removed leading to average offsets below 1.2 mm.

Experiment 2 introduces GTRPs as additional parameters to absorb the nadir-dependent variations to test the PVs. From the latter test, we may conclude that the PVs and PCOs are consistent for all GNSS and for both calibration methods. With an average GTRP offset below 1 mm, we may assume that the calibrations are mutually consistent and that they may be used to transform the scale from one GNSS to another.

The variation of the ISTP values is indicators for the consistency of different type-mean receiver antenna calibrations. The average ISTP values per antenna type for Experiments 1b and 2 as well as the GTRA in the case of the latter experiment are listed in Table 6. The values depend on the different antenna types and vary with the used calibration method. The ISTP and GTRP values for antenna *ASH701945C\_M NONE*, for robot and chamber calibrations, are above 2 cm. The antenna was used by 4 stations and revealed a poor daily repeatability. The robot calibrations showed a good consistency below 5 mm except for the antennas *JAVRINGANT\_DM NONE* and *TRM115000.00 NONE* with a discrepancy of  $-8$  mm and 5 mm, respectively. The chamber calibrations show a similar behavior. With the exception of the antennas *JAVRINGANT\_DM NONE* (discrepancy 9 mm), *JAVRINGANT\_G5T NONE* ( $-9$  mm), and *TRM59800.00 SCIS* ( $-5$  mm), all antennas show an average value below 5 mm. Overall, we may state that we have a good agreement between GPS and Galileo (and GLONASS)

**Table 6** Number of stations (#), Inter-system Translation Bias (ISTP) of Experiment 1b and ISTP and elevation dependent offset of Experiment 2 for each antenna/random combination using the Galileo scale for the satellite PCOs (experiment 2). Median values over the time period 2017–2018. Antennas which were observed less than 50 times (station and day) are not shown. Station MOBS is excluded due to data problem

Antenna experiment	CHA				ROB			
	1b		2		1b		2	
	#	ISTP	ISTP/	GTRA	#	ISTP	ISTP/	GTRA
ASH701945C_M NONE	4	-2.63	66.04/	-45.59	4	2.21	37.69/	-22.48
ASH701945E_M NONE					4	1.68	0.38/	0.54
JAVRINGANT_DM NONE	15	6.46	8.50/	-0.00	15	4.08	3.34/	0.66
JAVRINGANT_DM SCIS	1	2.92	0.82/	1.39	1	0.57	-7.92/	3.68
JAVRINGANT_G5T NONE	6	-1.94	-8.50/	2.22	6	2.54	-1.80/	1.49
JAV_RINGANT_G3T NONE	16	0.72	-1.87/	1.04				
LEIAR10 NONE	4	0.96	2.14/	-0.07	4	3.47	3.27/	0.35
LEIAR20 LEIM	4	-0.18	-1.77/	0.44	4	2.75	-0.32/	1.10
LEIAR20 NONE	4	-0.09	1.09/	0.23	4	2.21	2.02/	0.45
LEIAR25.R3 LEIT	17	2.97	4.74/	0.07	17	3.67	1.54/	1.06
LEIAR25.R3 NONE	5	-1.70	-4.62/	0.34	5	2.40	-1.12/	0.53
LEIAR25.R4 LEIT	12	0.36	-0.05/	0.69	12	0.45	-1.08/	0.97
LEIAR25.R4 NONE	7	0.68	0.57/	0.45	7	1.86	0.43/	0.64
LEIAT504 NONE					1	3.81	1.96/	0.42
SEPCHOKE_B3E6 NONE					1	0.16	-2.07/	1.46
SEPCHOKE_B3E6 SPKE					1	1.15	-1.01/	0.95
TPSCR.G3 NONE					2	3.99	0.94/	1.00
TPSCR.G3 SCIS					2	2.39	-1.23/	1.45
TPSCR.G3 TPSH					1	-1.22	-1.90/	0.23
TRM115000.00 NONE					5	2.92	5.42/	-0.74
TRM57971.00 NONE	17	0.44	1.64/	-0.86	17	-1.49	-0.13/	-0.86
TRM57971.00 TZGD	3	0.26	0.08/	-0.46	3	0.37	-0.09/	-0.20
TRM59800.00 NONE	29	-1.37	2.62	-0.72	31	-0.55	0.60/	-0.06
TRM59800.00 SCIS	14	-4.10	-5.10/	0.70	14	-1.80	-2.31/	0.38

among the antenna types as most of the offsets are in case of chamber calibrations below 4 mm and even below 3 mm for robot calibrations. The station-wise repeatability of the daily ISTP estimations of Experiments 1b and 2 are shown in Fig. 5. The average  $1 - \sigma$  scatter (derived from the 0.16 and 0.84 quantiles to be insensitive to outliers) of the ISTPs is about 2.6 mm for chamber calibrations and 2.7 mm for robot calibrations. Adding the GTRP parameter in Experiment 2 leads to a roughly 1.7 times larger scatter.

## 5 Scale and PCO determination

### 5.1 Scale estimation

After generating the 3-day NEQs based on the two calibration techniques (robot calibrations (ROB) and chamber calibrations (CHA)) for 2 years, we estimated the corresponding scales. We used NEQs which include, among other parameters, coordinates and PCOs. The orbits and Earth Rotation Parameters (ERP) were pre-eliminated. We estimated a GPS,

a Galileo (GAL) and a GLONASS (GLO) scale by constraining the corresponding PCOs in the NEQs to their a priori values. The coordinates were then compared to the ITRF 2014 coordinates using the reference sites only (outliers were removed during the datum definition) estimating three translations, three rotations and a scale. A positive scale means that the estimated coordinates are above the ITRF and a negative scale that the estimated coordinates are below.

Altamimi et al. (2016) showed that daily estimated VLBI scales show an annual sinusoidal patterns. The same characteristic is observed in the GNSS-derived scale parameters. Therefore, the overall scale was estimated in combination with an annual signal (a sine and a cosine term). The results are summarized in Table 7. In addition to our estimates, the table also contains the scale and the annual signal of the ITRF 2014, which is based on all available space techniques (Altamimi et al. 2016). The amplitude of about 0.3 ppb emerging from the GNSS techniques is similar to the amplitude resulting from the International VLBI Service for geodesy and astrometry (IVS, Nothnagel et al. 2017) but the GNSS-derived annual signal has a phase shift of about  $80^\circ$

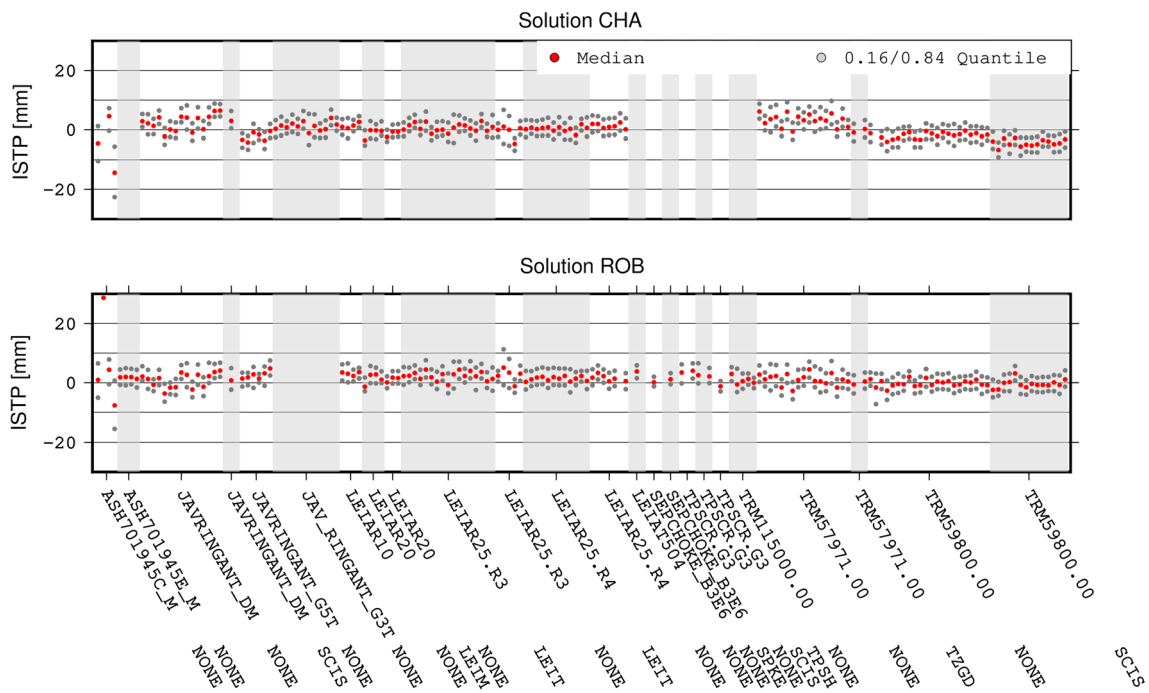


**Fig. 5** Median ISTP per station from Experiment 1b over the processed time period between 2017 and 2018. The scatter of the ISTPs are shown with the 0.16 and 0.84 quantiles ( $\pm\sigma$ )

w.r.t. the IVS solution. The solutions from the International Laser Ranging Service (ILRS, Pearlman et al. 2002) and the International DORIS Service (IDS, Willis et al. 2016) have smaller annual amplitudes. The seasonal amplitudes reflect mainly the loading effects and may differ due to different station distributions in the networks of the individual techniques (Collilieux et al. 2010; Altamimi et al. 2016). The RMS of the estimated scale is about 0.1 ppb. Figure 6 shows the time series of the scale estimated by constraining the Galileo PCOs for both solutions, ROB and CHA.

For the scale comparison between the ITRF2014 and the individual solutions, potential long-term drifts have to be taken into account. For SLR and VLBI, the drifts w.r.t. ITRF2014 are provided by Altamimi et al. (2016). The intrinsic drift for GNSS is primarily given by the consideration of PCOs which are assumed to be constant (Collilieux and Schmid 2013; Reischung and Schmid 2016). We assumed the scale drift to be close to the one between the igs14.atx-based GNSS solutions and the ITRF2014 with +0.026 ppb, leading to a total drift between 2010 and 2018 of 0.21 ppb (Reischung and Schmid 2016).

The ROB solution shows the expected behavior. Constraining the PCOs to GPS or GLONASS leads to a small-scale difference. This is due to the fact that the introduced IGS14 GPS and GLONASS PCOs are aligned to the ITRF2014 using robot calibrations. The scale difference w.r.t. ITRF2014 is 0.25 ppb, which is close to the expected difference of +0.21 ppb when taking the drift from the year

2010 onward into account. The Galileo scale is 1.41 ppb and would, reducing it by the rate of +0.026 ppb/year, be about 1.20 ppb in 2010. The PCOs for GPS and GLONASS are derived from the ITRF 2014 solution and should be consistent with the current ITRF scale. Figure 7 shows the daily scale estimations for SLR, VLBI and DORIS for the ITRF 2014 (Altamimi et al. 2016) and our estimated GNSS scale (using the drift presented in Reischung and Schmid (2016)).

The scale discrepancy between the GPS and the Galileo solution is 1.65 ppb for chamber calibrations. The ROB solution has a difference of 1.16 ppb. The RMS of the scale determination is the same in both solutions. Both solutions are internally fully consistent. Robot and chamber calibrations are not the same, however, and may have differences in the PCOs up to 7 mm. (Sect. 2.3). The IGS relies mostly on robot calibrations for its contribution to the ITRF as, in particular for older antenna types, only robot calibrations are available.

### 5.2 Phase center offset (PCO) estimation

The network scale is a function of the PCOs of the satellite and receiver antennas. If the receiver antennas are fully calibrated and if the PCOs for the satellites of one GNSS are available, we can transfer the scale of the GNSS with the known PCOs to the PCOs of the other constellations via the ground antennas. Introducing the PCOs of one GNSS defines the PCOs of all other GNSS, as well, via the scale of

**Table 7** Average scale in 2017–2018 considering a constant term and an annual signal (amplitude and phase) for GPS, GLONASS (GLO), and Galileo (GAL). IVS (VLBI), ILRS (SLR), and IDS (DORIS) values from Altamimi et al. (2016)

Solution	Scale [ppb]	Amplitude [ppb]	Phase [degree]	RMS [ppb]
CHA, GAL fixed	1.03	0.28	329	0.12
CHA, GPS fixed	-0.62	0.29	338	0.11
CHA, GLO fixed	-1.02	0.30	323	0.11
ROB, GAL fixed	1.41	0.31	328	0.12
ROB, GPS fixed	0.25	0.28	329	0.08
ROB, GLO fixed	0.20	0.30	316	0.09
IVS	0.68	0.28	245	
ILRS	-0.68	0.11	258	
IDS		0.06	204	

**Table 8** System-wise PCO offset estimates in cm constraining different PCOs. Two years of NEQs were stacked (2017–2018)

Fixed	CHA			ROB		
	GPS	GLO	GAL	GPS	GLO	GAL
GPS	-	-6.1	25.8	-	-0.3	21.9
GLO	4.0	-	31.6	-0.8	-	22.7
GAL	-22.1	-25.8	-	-15.0	-14.3	-

PCOs belonging to the ITRF are based on robot calibrations, and therefore, smaller discrepancies for the ROB solution are expected.

Figure 8 shows the system-wise PCO offset estimates for 2017–2018 for the ROB and CHA solutions. The annual signal can be seen when inducing the scale trough ITRF coordinates. Constraining the GPS or Galileo PCOs instead removes the annual signal, because it is absorbed by the coordinates. This can be observed in the scale determination of the individual solutions (Table 7). The scatter of the PCOs is small (CHA: 2.6 mm, ROB: 1.5 mm). For the ROB solution, more than 300 stations were used, only up to about 200 sites for the CHA solutions, which might explain the difference in scatter between the two solutions.

### 5.3 Summary

Our analysis shows that a GNSS-based scale can be extracted with a daily repeatability of 0.12 ppb. The Galileo scale w.r.t. ITRF2014, evaluated at the mean epoch of our experiment (January 1, 2018), is between 1.03 (CHA) and 1.41 (ROB) ppb. The annual variation in the scale over the two years is similar in amplitude to the one observed by the IVS, and it has a significant phase shift. The difference between the CHA and ROB solutions is 0.38 ppb, which may be caused by the different networks (multi-GNSS calibrations for different antenna types) and potential systematic errors in the calibrations. For GNSS, we are in the comfortable situation to have two independent types of calibrations available allowing it to compare them. We conclude that the Galileo scale can be used for GNSS solutions using calibrated ground receiver antennas. The procedure has the potential to contribute to a TRF scale. The selection of the receiver antennas is an important part of our method. For the sake of consistency, we propose to rely mainly on robot calibrations, because such a TRF contribution covers GNSS back to at least 1994. The PCO estimation by fixing Galileo leads to a change of -15.0 and -14.3 cm for GPS and GLONASS PCOs when using robot calibrations, and -22.1 and -25.8 cm for chamber calibrations. The formal error of the estimates, when stacking the NEQs of the years 2017 and 2018, is about 1.4 mm. Introducing the PCO corrections for GPS and GLONASS, according to Table 8 leads to a consistent set of PCOs which are in agree-

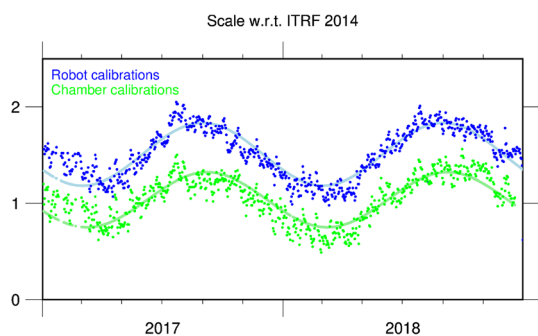


**Fig. 6** Scale introduced by Galileo using robot (blue) or chamber (green) calibrations. The light-blue and light-green curves represent the estimated scale for the period 2017–2018 consisting of a scale and an annual term (amplitude and phase)

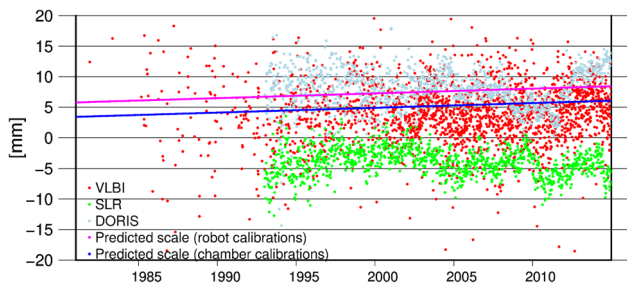


**Fig. 7** Scale w.r.t. ITRF 2014 for SLR, VLBI and DORIS (Altamimi et al. 2016). Scale predictions for the Galileo-induced scale using robot or chamber calibrations patterns assuming the same scale rate as for the IGS14 terrestrial frame w.r.t. ITRF 2014 (Rebischung and Schmid 2016)

the ground network. When constraining the a priori values for GPS (or GLONASS) PCOs, the GLONASS (or GPS) PCOs remain more less unchanged, whereas we see a discrepancy in the Galileo PCOs of about 20 cm (Table 8), documenting that the Galileo scale does not agree with the GPS/GLONASS PCOs derived from the ITRF. We can also observe a similar behavior between the robot and chamber calibrations. The

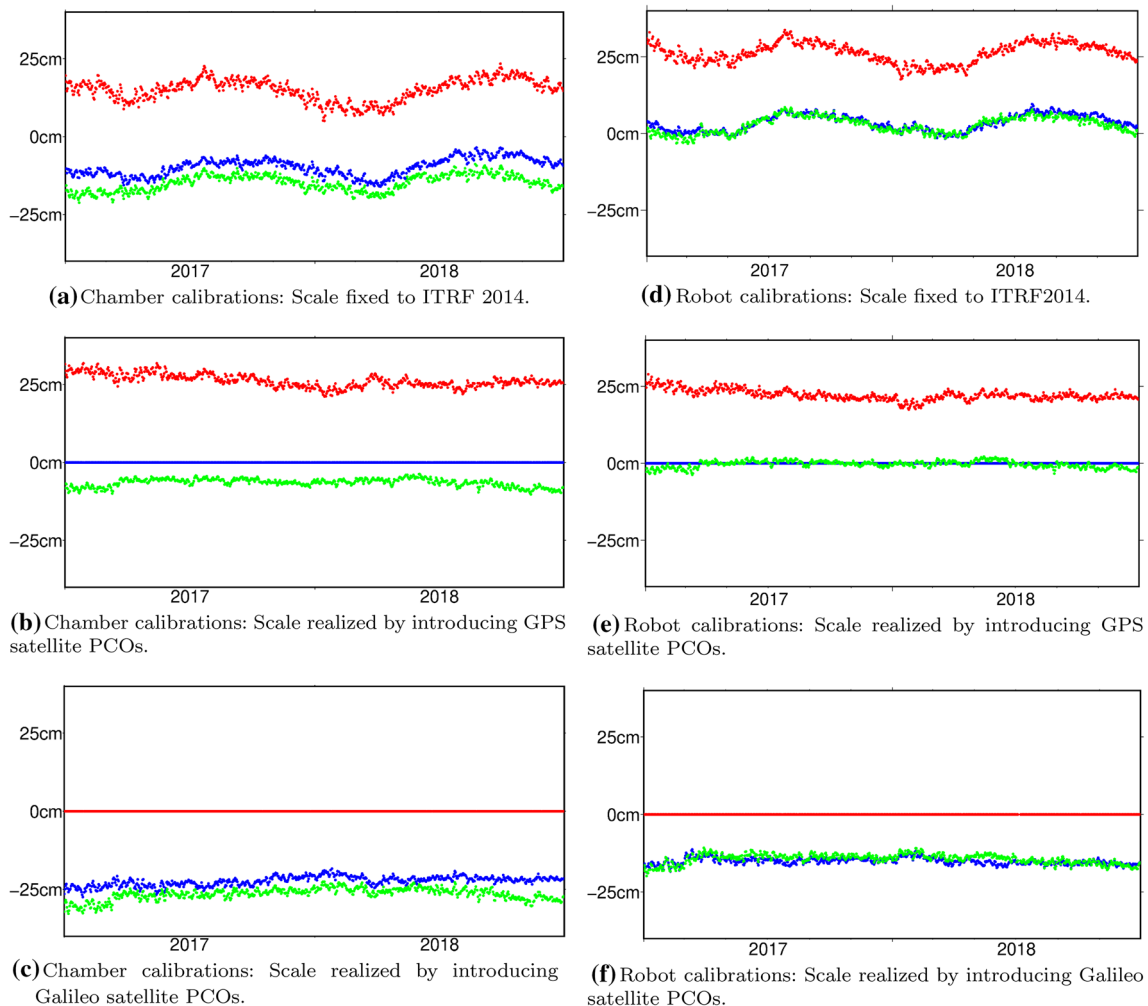


**Fig. 8** System-wise PCO estimation (z-component). Left: chamber-calibrated receiver antennas (based on up to 200 sites). Right: robot-calibrated receiver antennas (based on up to 300 sites). GPS: blue, GLONASS: green, Galileo: red

ment with the Galileo-induced scale. The resulting scale is at the mean epoch of our experiment (January 1, 2018) for the CHA solution  $1.03 \pm 0.12$  ppb with a yearly amplitude of 0.28 ppb. In case of ROB, the scale is  $1.41 \pm 0.12$  ppb with a yearly amplitude of 0.31 ppm. The daily scale estimates are almost identical to the solution where only the Galileo PCOs are constrained and system-wise PCO offsets are estimated, as shown in Fig. 6.

## 6 Conclusions

The scale determination of the ground tracking network with GNSS became feasible with the disclosure of the Galileo satellite antenna patterns on April 25, 2019 and with the availability of multi-GNSS calibrations for receiver antennas. At present, two sources of receiver antenna calibrations are available. Robot and chamber calibrations support mean-

while the Galileo system and can be used in future IGS contributions to new ITRF releases. Robot and chamber calibrations show overall small discrepancies in the derived PCOs and the network scale. Robot calibrations are closer to the current ITRF 2014 solution.

A GNSS TRF scale may be derived relying on either robot or chamber calibrations. The Galileo scale difference w.r.t. ITRF2014, evaluated at the mean epoch of our experiment (January 1, 2018), is 1.4 ppb in case of robot and 1.0 ppb in case of chamber calibrations. The VLBI scale difference for January 1, 2018, is taking the drift into account, 0.84 ppb. The extrapolated scale of the ILRS solution is  $-0.84$  ppb.

ISTP may be used to test the compatibility of different GNSS antenna calibrations for individual ground antennas and to check the consistency of the individual GNSS scales induced by their PCOs. Using the chamber-calibrated Galileo satellite antenna pattern together with the IGS14 PCOs of GPS and GLONASS will introduce and average

offset between GPS/GLONASS and Galileo of about 7 mm. After re-adjusting the PCOs to the Galileo scale, the ISTP are reduced, as expected, to roughly 1 mm. The Galileo ISTP values for the individual type mean antennas show a scatter of about 3 mm.

Introducing known PCOs from at least one GNSS, e.g., Galileo, is sufficient to estimate the network scale and to adjust the PCOs of the other GNSS accordingly. The question remains, however, whether the Galileo scale may be transferred backwards in time using GPS and GLONASS PCOs. This could be achieved by using the estimated PCOs and introduce the values from 2017–2018 to time periods with no or only limited Galileo constellation. It would be much better, however, if calibrated GPS and GLONASS PCOs would be disclosed in analogy to those of Galileo.

**Acknowledgements** We are grateful to Zuheir Altamimi for providing the time series of the scale differences between the individual SLR and VLBI solutions and the ITRF 2014. This research was supported by the European Research Council under the Grant agreement No. 817919 (project SPACE TIE). All views expressed are those of the authors and not of the European Research Council.

**Author contributions** A.V. and R.D. designed the research; A.V. performed the research and designed the paper; A.V., R.D., and S.S. analyzed the data; L.P. contributed to the data analyzes; F.Z. and H.K. contributed the receiver antenna chamber calibrations, M.S. and G.W. contributed the receiver antenna robot calibrations; A.J. and G.B. substantially contributed to the interpretation of results and provided many useful suggestions in the internal review process.

**Funding** Open access funding provided by University of Bern.

**Data availability** The NEQs of our two solutions (ROB and CHA) are available in the SINEX file format on our ftp server ([ftp://ftp.aiub.unibe.ch/users/villiger/scale\\_repro/](ftp://ftp.aiub.unibe.ch/users/villiger/scale_repro/)).

**Open Access** This article is licensed under a Creative Commons Attribution 4.0 International License, which permits use, sharing, adaptation, distribution and reproduction in any medium or format, as long as you give appropriate credit to the original author(s) and the source, provide a link to the Creative Commons licence, and indicate if changes were made. The images or other third party material in this article are included in the article's Creative Commons licence, unless indicated otherwise in a credit line to the material. If material is not included in the article's Creative Commons licence and your intended use is not permitted by statutory regulation or exceeds the permitted use, you will need to obtain permission directly from the copyright holder. To view a copy of this licence, visit <http://creativecommons.org/licenses/by/4.0/>.

## References

- Altamimi Z, Rebischung P, Mtivier L, Collilieux X (2016) ITRF2014: a new release of the International Terrestrial Reference Frame modeling nonlinear station motions. *J Geophys Res Solid Earth* 121(8):6109–6131
- Arnold D, Meindl M, Beutler G, Dach R, Schaer S, Lutz S, Prange L, Sońnica K, Mervart L, Jäggi A (2015) CODE's new solar radiation pressure model for GNSS orbit determination. *J Geod* 89(8):775–791
- Böhm J, Werl B, Schuh H (2006) Troposphere mapping functions for GPS and VLBI from ECMWF operational analysis data. *J Geophys Res* 111(B2):B02406
- Bruni S (2016) Combination of GNSS and SLR measurement: contribution to the realization of the terrestrial reference frame. PhD thesis, Astrophysics [astro-ph]. PSL Research University. NNT : 2016PSLEO001 . tel-01428831
- CAO (2017) QZSS Satellite Information. <https://qzss.go.jp/en/technical/qzssinfo/index.html> accessed 2019-11-1
- Chen G, Herring TA (1997) Effects of atmospheric azimuthal asymmetry on the analysis of space geodetic data. *J Geophys Res* 102(B9):20489–20502
- Collilieux X, Altamimi Z, Coulot D, Van Dam T, Ray J (2010) Impact of loading effects on determination of the international terrestrial reference frame. *Adv Space Res* 45:144–154
- Collilieux X, Schmid R (2013) Evaluation of the ITRF2008 GPS vertical velocities using satellite antenna z-offsets. *GPS Solution* 17(2):237–246
- Dach R, Lutz S, Walser P, Fridez P (2015) Bernese GNSS Software Version 5.2. University of Bern, Bern Open Publishing
- Dach R, Schaer S, Arnold D, Prange L, Sidorov D, Stebler P, Villiger A, Jäggi A (2017) CODE final product series for the IGS. Published by Astronomical Institute, University of Bern, Bern
- GSA (2019) Galileo IOV and FOC satellite metadata. <https://www.gsc-europa.eu/support-to-developers/galileo-iov-satellite-metadata> Accessed 2018-01-26
- Haines BJ, Bar-Sever YE, Bertiger WI, Desai SD, Harvey N, Siboso AE, Weiss JP (2015) Realizing a terrestrial reference frame using the global positioning system. *J Geophys Res Solid Earth* 120(8):5911–5939
- Johnston G, Riddell A, Hausler G (2017) The International GNSS service. In: Teunissen PJ, Montenbruck O (eds) Springer handbook of global navigation satellite systems. Springer, Cham, Switzerland, pp 967–982
- Lutz S, Meindl M, Steigenberger P, Beutler G, Sońnica K, Schaer S, Dach R, Arnold D, Thaller D, Jäggi A (2016) Impact of the arc length on GNSS analysis results. *J Geod* 90(4):365–378
- Menge F, Seeber G, Völksen C, Wübbena G, Schmitz M (1998) Results of absolute field calibration of GPS antenna PCV. In: Proceedings of the ION GPS-98, Nashville, Tennessee
- Nothnagel A, Artz T, Behrend D, Malkin Z (2017) International vlbi service for geodesy and astrometry. *J Geodesy* 91(7):711–721
- Pearlman M, Degnan J, Bosworth J (2002) The international laser ranging service. *Adv Space Res* 30(2):135–143
- Petit G, Luzum B, (2010). IERS conventions, (2010) IERS Technical Note 36. Bundesamt für Kartographie und Geodäsie, Frankfurt a. M
- Prange L, Villiger A, Sidorov D, Schaer S, Beutler G, Dach R, Jäggi A (2020) Overview of CODE's MGEX solution with the focus on Galileo. *Adv Space Res*. <https://doi.org/10.1016/j.asr.2020.04.038>
- Ray JR, Rebischung P, Schmid R (2013) Dependence of IGS products on the ITRF datum, in REFAG 2014, International Association of Geodesy, vol. 146, edited by T. van Dam, Springer, Berlin, In: Proceedings of the IAG Commission 1, Kirchberg (Luxembourg), 13–17 October, 2014, <https://doi.org/10.1007/978-3-319-45629-4>
- Rebischung P (2014) Can GNSS contribute to improving the ITRF definition? PhD thesis, PhD thesis, Observatoire de Paris
- Rebischung P, Schmid R (2016) IGS14/igs14.atx: a new framework for the IGS products. AGU Fall Meeting, San Francisco, CA., <https://mediatum.ub.tum.de/doc/1341338/file.pdf> (accessed 2020-05-01)

- Rodriguez-Solano CJ, Hugentobler U, Steigenberger P, Lutz S (2012) Impact of Earth radiation pressure on GPS position estimates. *J Geod* 86(5):309–317
- Schmid R, Dach R, Collilieux X, Jäggi A, Schmitz M, Dilssner F (2016) Absolute IGS antenna phase center model igs08.atx: status and potential improvements. *J Geod* 90(4):343–364
- Schmid R, Steigenberger P, Gendt G, Ge M, Rothacher M (2007) Generation of a consistent absolute phase-center correction model for gps receiver and satellite antennas. *J Geod* 81(12):781–798
- Steigenberger P, Fritsche M, Dach R, Schmid R, Montenbruck O, Uhlemann M, Prange L (2016) Estimation of satellite antenna phase center offsets for Galileo. *J Geod* 90(8):773–785
- Willis, P., Lemoine, F. G., Moreaux, G., Soudarin, L., Ferrage, P., Ries, J., Otten, M., Saunier, J., Noll, C., Biancale, R., and Luzum, B. (2016). The International DORIS Service (IGS): Recent developments in preparation for ITRF2013. In: Rizos, C. and Willis, P., editors, IAG 150 Years, pp. 631–640, Cham. Springer
- Wübbena, G., Schmitz, M., Menge, F., Böder, V., and Seeber, G. (2000). Automated Absolute Field Calibration of GPS Antennas in Real-Time. In: Proceedings of the ION GPS-00, Salt Lake City, Utah
- Wübbena G, Schmitz M, Menge F, Seeber G, Vöölksen C (1997) A new approach for field calibration of absolute GPS antenna phase center variations. *Navigation* 44(2):247–255
- Zeimetz P, Kuhlmann H (2008) On the accuracy of absolute GNSS antenna calibration and the conception of a new anechoic chamber. In: Proceedings of the FIG working week, Stockholm, Sweden, June 14–19, 2008
- Zhu SY, Massmann F-H, Yu Y, Reigber C (2003) Satellite antenna phase center offsets and scale errors in gps solutions. *J Geod* 76(11):668–672